

A close relationship at $z \sim 2$: submillimetre galaxies and BzK-selected galaxies^{*}

Toshinobu Takagi^{1†}, Yoshiaki Ono², Kazuhiro Shimasaku², Hitoshi Hanami³

¹ *Institute of Space and Astronautical Science, Japan Aerospace Exploration Agency, Sagamihara, Kanagawa 229 8510, Japan*

² *Department of Astronomy, School of Science, University of Tokyo, Tokyo 113-0033, Japan*

³ *Physics Section, Faculty of Humanities and Social Sciences, Iwate University, Morioka, 020-8550, Japan*

ABSTRACT

We investigate the relationship between two massive star-forming galaxy populations at redshift $z \sim 2$; i.e. submillimetre galaxies (SMGs) and BzK-selected galaxies (BzKs). Out of 60 SMGs found in the Subaru/XMM-Newton deep field, we collect optical–NIR photometry of 28 radio counterparts for 24 SMGs, based on refined sky positions with a radio map for 35 SMGs (Ivison et al. 2007). We find a correlation between their K -band magnitudes and $BzK [\equiv (z - K) - (B - z)]$ colours: almost all of the K -faint ($K_{AB} > 21.3$) radio-detected SMGs have $BzK > -0.2$, and therefore BzKs. This result gives strong support to perform direct optical identification of SMGs by searching for BzKs around SMGs. We calculate the formal significance (P' value) for each of the BzK associations around radio-undetected SMGs, and find 6 new robust identifications, including one double identification. From this analysis, we obtain the current best estimate on the surface density of BzK-selected SMGs, which indicates that only ~ 1 per cent of BzKs are SMGs. If BzKs are normal disk-like galaxies at $z \sim 2$ as indicated by the correlation between their star formation rate (SFR) and stellar mass and also by dynamical properties, SMGs are likely to be merging BzKs. In this case, a typical enhancement of SFR due to merging is only a factor of ~ 3 , which is an order of magnitude lower than that of local ULIRGs. This may indicate that most of the merging BzKs could be observed as SMGs. Considering a possible high fraction of mergers at $z \sim 2$ (at least it would be higher than the fraction at $z \lesssim 1$ of ~ 10 per cent), it is rather puzzling to find such a low fraction of SMGs in the progenitor population, i.e. BzKs.

Key words: galaxies: starburst – dust, extinction – infrared: galaxies – submillimetre – galaxies: evolution.

1 INTRODUCTION

Among many cosmological surveys, the submillimetre (submm) survey is very unique, in the sense that the expected flux density of sources is almost insensitive to redshift for $z \approx 1 - 8$, owing to the strong negative K -correction (e.g. Blain et al. 2002). Although the current sensitivity allows us to detect only the brightest infrared galaxies in the universe, it is possible to detect massive starbursts and gas rich QSOs at extreme redshifts $z \gg 6$ if exist (e.g. Priddey et al. 2008). However, most of the submm galaxies (SMGs) currently identified lie at $z \lesssim 3$. This is not because of the detection limit as noted above, but because of the ‘identification limit’, owing to a large beam size of current (sub)mm telescopes used for surveys. The radio emission provides a

high-resolution substitute for the infrared emission observed in the submm (e.g. Chapman et al. 2001, 2003; Ivison et al. 2002; Borys et al. 2004; Dannerbauer et al. 2004; Ivison et al. 2007), and hence the detection limit in the radio has set the upper limits on redshifts of identified SMGs (Chapman et al. 2005). The best way to identify optical counterparts of SMGs is to have high resolution submm images with interferometers (Iono et al. 2006; Younger et al. 2007; Wang et al. 2007; Dannerbauer et al. 2008). Although time consuming, it allows us to perform direct optical/near-infrared (NIR) identifications from the submm position.

Here we adopt another method of direct optical identification using optical/NIR colours of galaxies around the submm source. The expected number of random optical/NIR associations within the error circle of the submm position is not negligible; e.g. there would be ~ 4 K -band sources ($K_{AB} < 23$) on average within a $r < 8''$ radius

† E-mail: takagi@ir.isas.jaxa.jp

(see below). However, if SMGs have rather confined optical-NIR colours and the surface density of objects with similar colours is reasonably low, it will be possible to directly identify SMGs without using costly high-resolution submm images. As in the radio identification method (Downes et al. 1986), we can calculate the formal significance of each optical/NIR association, given the number counts of colour-selected galaxies. To do this we need a firm basis for the colours of SMGs.

Since the discovery of SMGs, extremely red objects (EROs) usually defined with $(I - K)_{\text{Vega}} \gtrsim 4$ or $(R - K)_{\text{Vega}} \gtrsim 5$ and distant red galaxies with $(J - K)_{\text{Vega}} > 2.3$ have been paid special attention as candidates of SMG counterparts (e.g. Smail et al. 1999, 2002; Webb et al. 2003; Coppin et al. 2004; Frayer et al. 2004; Clements et al. 2004; Pope et al. 2005). It turns out that the fraction of EROs or DRGs in SMGs is not very high and their surface densities are not low enough to reject random associations. Among the NIR-selected galaxy populations in the literature, BzK-selected star-forming galaxies (BzKs – Daddi et al. 2004) may be the most promising counterparts of SMGs (Reddy et al. 2005; Bertoldi et al. 2007; Takagi et al. 2007), which lie at $1.4 \lesssim z \lesssim 2.5$ and include heavily obscured galaxies, such as SMGs, as an extreme subset.

In this paper, we indeed find that almost all of the K -faint (indicating higher redshifts) radio-detected SMGs are BzKs. We then use BzKs as a key galaxy population to identify radio-undetected SMGs at $1.4 \lesssim z \lesssim 2.5$. Since the BzK-selection is based on observed wavelengths covering a spectral break at 4000 \AA , we can naturally extend this selection technique to the higher redshift range, e.g. $z \gg 3$, in the future by using a combination of wavebands at longer wavelengths. We also emphasize that the understanding of the physical relation between SMGs and BzKs would be important to reveal the evolution of galaxies at $z \sim 2$, given that they have similar stellar masses of $\sim 10^{11} M_{\odot}$, and spatial correlation lengths of $\sim 10 h^{-1} \text{ Mpc}$ (Blain et al. 2004; Kong et al. 2006; Hayashi et al. 2007). We discuss the hypothesis of SMGs being merging BzKs.

We adopt the sample of SMGs from the SCUBA HALF Degree Extragalactic Survey (SHADES – Mortier et al. 2005; Coppin et al. 2006) as described in Section 2. In Section 3, we investigate typical optical/NIR colours of the radio-detected SMGs. We apply our direct identification method for radio-undetected SMGs in Section 4. We then discuss a possible evolutionary link between SMGs and BzKs in Section 5. Finally we give our summary in Section 6. Throughout this paper, we assume a cosmology with $\Omega_{\text{m}} = 0.3$, $\Omega_{\Lambda} = 0.7$ and $H_0 = 70 \text{ km sec}^{-1} \text{ Mpc}^{-1}$. All magnitudes in this paper use the AB system unless otherwise noted.

2 DATA AND SAMPLE

2.1 SMGs with radio identification

The sample of SMGs is taken from the SHADES source catalogue in the Subaru/XMM-Newton Deep Field (SXDF), which contains 60 reliable sources (Coppin et al. 2006). Ivison et al. (2007) found robust 41 radio associations for 35 SMGs. They calculated the formal significance of each of

the potential submm/radio associations, by correcting the raw Poisson probability with the method of Downes et al. (1986). A submm/radio association is regarded as being robust if the corrected Poisson probability P' is less than 0.05 with a search radius of $8''$. The detection limit at 1.4 GHz is $6.7 \mu\text{Jy beam}^{-1}$ in the best region (1σ ; Ivison et al. 2007) with a FWHM of $1.7''$.

One of the SMGs, SXDF850.6, has a triple radio association, 2 robust and 1 tentative. A high angular resolution image with Submillimetre Array (SMA) pinned down the tentative radio association as a true radio counterpart (J. Dunlop et al., private communication). Thus, two ‘robust’ radio associations happen by chance. Excluding these two chance associations, and adding the true radio counterpart of SXDF850.6, we investigate 40 radio associations in total. Ivison et al. (2007) also suggest one $24 \mu\text{m}$ source as a counterpart of SXDF850.71, which has no radio associations. We also include this MIR counterpart in the analysis below. However, this source is eventually excluded in our study, since we find no reliable K_s -band counterpart within a search radius of $2''$.

2.2 Optical – NIR counterparts

We search for optical and NIR counterparts of 40 radio and 1 MIR sources with a search radius of $2''$, using the official optical source catalogue of SXDS (ver.1 – Furusawa et al. 2008) and the NIR source catalogue of UKIDSS data release 2. Here we concentrate on the sources detected in the K_s band only. The detection limits in the J and K_s bands are 22.61 and 21.55 mag (5σ in Vega; Warren et al. 2007), respectively. In the case of a multiple association for a radio source, we adopt the closest K_s -band source to the radio position as the correct optical-NIR counterpart. Some optical counterparts from the SXDS catalogue are found to be different from the NIR counterparts (mostly due to confusion of optical sources). In this case, we perform aperture photometry at the position of NIR sources.

We use matched aperture photometry with a $2''$ diameter to determine colours. However, when single K_s -band magnitudes are quoted they are total magnitudes (Petrosian magnitudes in the UKIDSS catalogue). We correct optical photometry for the galactic cirrus absorption. We note that SXDF850.21 is obviously a nearby galaxy with a large angular size, $\sim 30''$. For this galaxy, we measure optical/NIR colours from total magnitudes.

Using the UKIDSS/UDS catalogue, we find K_s -band counterparts for 29 radio sources out of 40. For SXDF850.6 (with the SMA identification), we find a K_s -band counterpart at $0.19''$ away from the radio position, but we find no optical counterpart, although it is very close to an optical source $\sim 1.5''$ away. This case is similar to three other SMGs discussed in Smail et al. (2004 – see their Figure 3). Excluding this complicated case, we obtain optical-NIR photometry of 28 radio counterparts for 24 SHADES sources in the SXDF. No K_s -band source is found at the position of the MIR counterpart of SXDF850.71. Out of the 28 K_s -detected radio sources, 20 are singly associated with the SHADES sources (hereafter singly associated SMGs). Therefore, these are the most reliable optical counterparts of SMGs.

The mean separation between radio and optical positions is $0.51'' \pm 0.07''$ with a maximum of $1.55''$

Table 1. Photometry of radio-detected SMGs

Name	R.A. [J2000]	Dec.	K_s [AB] ^a	$z' - K_s$	$B - z'$ [AB] ^b	$R - K_s$	$J - K_s$
SXDF850.01	34.37758	-4.99355	22.01±0.07	2.59	1.60	3.46	2.54
SXDF850.02	34.51490	-4.92432	21.50±0.04	2.61	1.11	2.95	2.13
SXDF850.03	34.42561	-4.94124	18.77±0.01	1.02	2.92	1.71	0.55
SXDF850.04	34.41116	-5.06093	21.04±0.03	2.83	1.43	3.54	1.37
SXDF850.05	34.51192	-5.00856	20.34±0.01	2.26	2.55	4.05	1.50
SXDF850.07	34.41192	-5.09108	21.22±0.03	2.67	1.30	3.12	1.75
SXDF850.08	34.43402	-4.93019	22.95±0.10	3.59	0.44	3.64	≥ 0.41 ^c
SXDF850.10	34.60375	-4.93423	21.93±0.05	2.14	1.41	2.69	1.60
SXDF850.12	34.49710	-5.08446	22.42±0.05	1.19	2.06	1.64	0.90
SXDF850.16	34.55784	-4.96193	21.84±0.03	2.39	1.10	3.17	1.07
SXDF850.19	34.61584	-4.97691	21.53±0.04	2.25	1.45	3.17	0.96
SXDF850.21 ^d	34.42711	-5.07356	15.51±0.01	0.33	0.85	0.53	-0.18
SXDF850.23	34.42679	-5.09602	23.54±0.12	2.67	0.49	3.15	1.35
SXDF850.24b	34.39473	-5.07499	20.74±0.02	2.24	2.53	3.51	1.16
SXDF850.27	34.53304	-5.02927	21.85±0.03	3.01	1.61	3.91	1.33
SXDF850.28a	34.52867	-4.98692	19.20±0.01	2.13	3.26	3.33	1.13
SXDF850.28b	34.52839	-4.98821	20.73±0.01	2.25	2.95	3.99	1.23
SXDF850.30	34.41660	-5.02102	21.37±0.03	3.95	2.70	5.29	2.07
SXDF850.31	34.39938	-4.93208	19.71±0.01	1.92	2.85	3.00	1.09
SXDF850.35	34.50349	-4.88503	19.68±0.01	1.91	2.22	3.04	1.04
SXDF850.37	34.35240	-4.97823	22.09±0.07	3.46	1.32	4.35	≥ 0.73 ^c
SXDF850.47a	34.39322	-4.98260	21.00±0.02	2.02	3.52	4.03	0.97
SXDF850.47b	34.39337	-4.98329	21.18±0.02	1.69	2.04	2.89	0.97
SXDF850.47c	34.39039	-4.98269	19.76±0.01	2.13	1.79	3.27	0.93
SXDF850.52a	34.52133	-5.08157	19.12±0.01	1.02	1.70	1.47	0.61
SXDF850.52b	34.52065	-5.08368	21.49±0.02	2.88	3.18	4.83	1.55
SXDF850.77	34.40069	-5.07595	20.35±0.01	1.95	3.12	3.36	1.12
SXDF850.96	34.50083	-5.03784	22.07±0.04	1.73	0.99	2.41	1.03

Note — ^a Total (Petrosian) magnitudes from the UKIDSS/UDS catalogue. ^b Aperture-matched ($2''$) colours, corrected for galactic extinction. ^c 5σ upper limit in J . ^d A nearby galaxy with large angular size. Colours are derived from total magnitudes.

(SXDF850.52a, an apparently large galaxy with $2''$ radius). See also Clements et al. (2008) for discussions on optical identifications of the same SHADES sources, in which the goodness of the SED fitting is taken into account. Our identifications of corresponding radio sources are consistent with those by Clements et al. (2008).

We convert J and K_s Vega magnitudes in the UKIDSS catalogue to AB magnitudes with $J[\text{AB}] = J[\text{Vega}] + 0.889$ and $K_s[\text{AB}] = K_s[\text{Vega}] + 1.857^1$. In order to achieve the same colour selection of galaxies as done in Daddi et al. (2004), we correct both $B - z'$ and $z' - K_s$ colours, based on the analysis of Takagi et al. (2007); i.e. we adopt $(B - z)_{\text{corr}} = (B - z') + 0.2$ and $(z - K)_{\text{corr}} = (z' - K_s) - 0.2$. Hereafter $(z - K)$ and $(z - K)$ denote the corrected AB colours.

¹ These conversion factors have been derived from the comparison of two catalogues for the same objects in SXDF; one is the UKIDSS/UDS catalogue in the Vega system, another is the one used in the analysis similar to this study by Takagi et al. (2007), originally from the observation with the University of Hawaii 2.2 m telescope with the Simultaneous 3-colour InfraRed Imager for Unbiased Survey (SIRIUS; Nagayama et al. 2003).

2.3 Additional sample from the literature

In order to give additional support to our results from the SHADES/SXDF sample, lacking spectroscopic redshifts so far, we also analyse the SMG sample in the Hubble Deep Field (HDF; Pope et al. 2005) with spectroscopic redshifts. For this HDF sample, we adopt B - and z' -band photometry of the Subaru/Suprime-cam (Capak et al. 2004) and K_s -band photometry from Pope et al. (2005). The colours are given by matched aperture photometry again, but with a $3''$ diameter as adopted in Pope et al. (2005). We apply the same colour correction as done for the SHADES sample to use the BzK selection criteria, since the photometric bands employed are the same. We find that seven SMGs in the HDF have BzK colours as well as spectroscopic redshifts. In Section 5, we use a larger sample of SMGs from Chapman et al. (2005), including SMGs in the HDF. Unfortunately, we can not use this large sample in the main analysis, since we find no z' -band photometry for the sample as a whole in the literature.

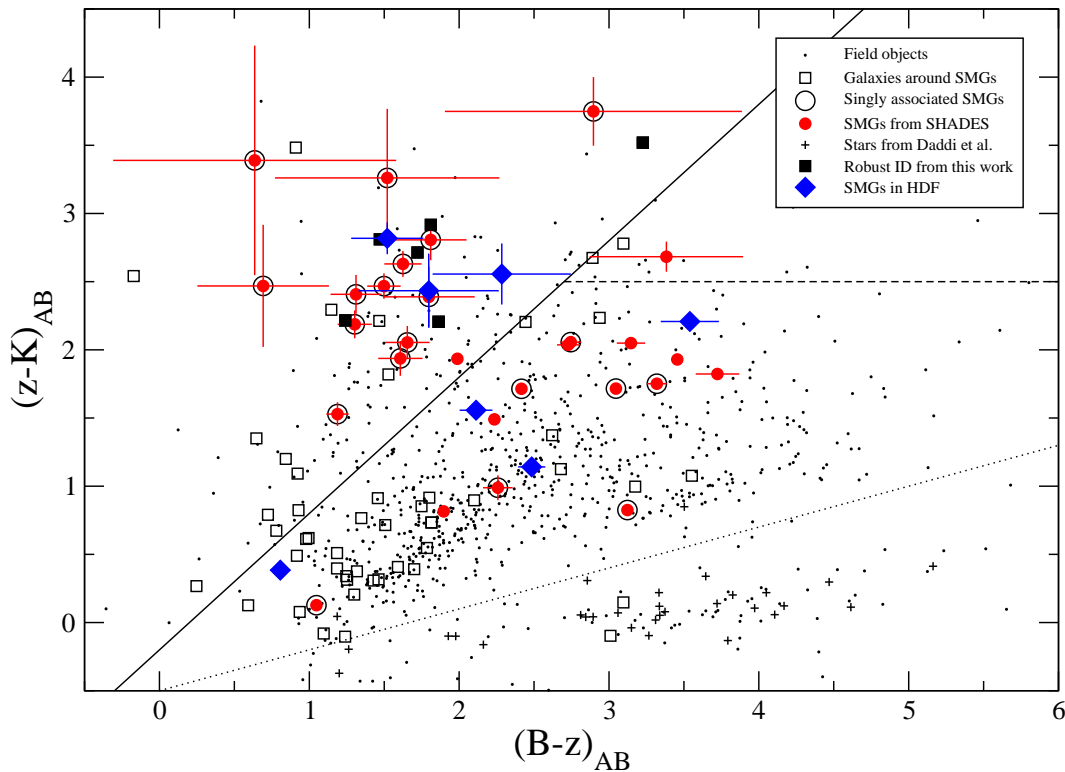


Figure 1. The BzK colour-colour diagram. Solid circles indicate radio-detected SMGs. Encircled ones are singly associated SMGs. Diamonds are the HDF sample from Pope et al. (2005). Field objects are K -band sources in the SXDF/SIRIUS field presented in Takagi et al. (2007). Squares indicate K -band sources within $8''$ radius from radio-undetected SMGs. Filled squares indicate robust NIR identification given in Section 4. Stars from Daddi’s catalogue are plotted as small pluses, which are used to calibrate the colour correction.

Table 2. Surface density of various NIR galaxy populations with $K_s < 23$

Population	Surface density [arcmin $^{-2}$]	Number per 8-arcsec radius
K -band sources ^a	64.75	3.61
BzKs ^b	7.13	0.39
EROs ^b	3.77	0.21
DRGs ^c	3.35	0.18
RK /BzKs ^b	1.49	0.083
RJK /BzKs ^d	0.75	0.04

References — ^aMaihara et al. (2001), ^bMotohara et al. (in prep.), ^cKajisawa et al. (2006), ^dAssumed to be half of RK /BzKs.

3 OPTICAL-NIR COLOURS OF SMGS

3.1 Relation with BzKs

Figure 1 shows the $B - z$ and $z - K$ colours of 28 radio counterparts of SMGs in the SXDF including multiple associations, and 7 SMGs in the HDF. A half $(14/28)^2$ satisfy the colour selection criteria for star-forming galaxies at

² Statistics on SMGs are evaluated for the SXDF sample only, because the noise level of the 850- μ m survey is uniform in the SXDF, and is not in the HDF.

$1.4 < z < 2.5$, i.e. $BzK > -0.2$, corresponding to an upper left corner in the BzK diagram. Out of the 20 singly associated SMGs, 13 ($65 \pm 10\%$) are classified as BzKs.

The BzK-selected SMGs have, on average, $(B - z) = 1.5$, and $(z - K) = 2.5$. Note that the BzK-selected SMGs are confined within colour ranges of $1 \lesssim (B - z) \lesssim 2$ and $1.5 \lesssim (z - K) \lesssim 3$. Not only SMGs, but also UV-selected (BX/BM) galaxies and DRGs have a large overlap with BzKs. While BzKs have $\langle z - K \rangle = 1.61$, BX/BM galaxies and DRGs have $\langle z - K \rangle = 1.07$ and 2.49, respectively (Reddy et al. 2005). If BzKs with $(z - K) > 3$ are mostly passively evolving galaxies as suggested by Reddy et al. (2005), SMGs are the reddest star-forming galaxies at $z \sim 2$ as expected from their high submm fluxes, indicating a large dust mass and attenuation.

On the other hand, Chapman et al. (2005) found that many of their SMG sample do occupy the BX/BM $z \sim 2$ colour, selection region in the $(U - g)$ - $(g - R)$ diagram, while SMGs are systematically redder in the BzK colours than BX/BM galaxies. This may suggest that complex gas/stellar geometry plays a role: when the main body of galaxies is heavily obscured, a small fraction of less obscured star-forming regions or individual stars can dominate the rest-frame UV fluxes and control the UV colours, while the rest-frame optical colours are determined by obscured, but still dominant light from the main body. Therefore, it is not unreasonable to find galaxies with blue UV and red optical/NIR colours (e.g. Takagi et al. 2003).

As indicated by the error bars in the BzK diagram, most of the BzK-selected SMGs belong to an optically fainter sample of SMGs. In order to emphasize this point, we show the histogram of BzK (along with $R-K$ and $J-K$) of the singly associated SMGs in Figure 2. In these histograms, hatched ones indicate K -faint ($K_s > 21.3$) radio-detected SMGs. The distribution of BzK is clearly bimodal. This may suggest that BzK-selected SMGs have a distinct spectral break at 4000 \AA , i.e. the Balmer break as suggested by Smail et al. (2004). We find that 14 singly associated SMGs out of 20 have $K_s > 21.3$. Therefore, 93 ± 6 per cent (13/14) of the singly associated K -faint SMGs are BzKs. The HDF sample also follows the same trend.

A high fraction of BzKs in K -faint SMGs is implied by the results of Takagi et al. (2007), using a sub-sample of the SHADES sources. Also, Bertoldi et al. (2007) derived a high fraction of BzKs in MAMBO 1.2 mm-detected galaxies in the COSMOS field. They found that 8/11 (73 ± 13 %) of robust radio counterparts are clearly BzKs. One possible difference between the MAMBO and SHADES sources could be the fraction of non-BzKs in the samples. A half of the radio counterparts of SMGs are non-BzKs, while the MAMBO counterparts include only a small fraction of non-BzKs, less than $\sim 20\%$ ($< 2/11$). Since most of the reliable MAMBO counterparts in Bertoldi et al. (2007) are faint in the K band (> 21.3), the difference between MAMBO and SHADES sources could be explained by the lack of K -bright galaxies in MAMBO counterparts (see also Dannerbauer et al. 2004). This might reflect a systematic difference in the redshift distribution between submm ($850 \mu\text{m}$) and millimetre (1.2 mm) sources. This should be tested with more reliable and statistically significant (sub)mm surveys with next generation instruments.

As expected from the bimodal distribution of the BzK colours in Figure 2, there is a correlation between BzK colours and K -band magnitudes. In Figure 3, we show this correlation along with expected colours and magnitudes of Arp220 and M82, well known nearby dusty galaxies. In order to match the SED templates of these two galaxies to the observed trend, their bolometric luminosities are multiplied by 2 and 20, resulting in 4×10^{12} and $8 \times 10^{11} L_\odot$ for Arp220 and M82, respectively. Both SED templates are consistent with the observed colour-magnitude relation of SMGs, indicating that the difference in K_s -band magnitudes originates mainly from redshift variations. According to the SED templates, K -faint ($K_s > 21.3$), BzK-selected SMGs are likely to be at $z \gtrsim 1.5$. As originally claimed by Daddi et al. (2004), the colour criterion of $BzK > -0.2$ would be useful to select galaxies having an obscured SED such as Arp220 or M82 at $z \gtrsim 1.4$.

A rough correlation between the apparent K -band magnitudes and redshifts of SMGs (Serjeant et al. 2003; Smail et al. 2004) also indicates that K -faint SMGs have systematically higher redshifts. In Figure 4, we show the BzK colour versus redshift for our SMGs. The redshifts of the HDF sample are spectroscopic ones, while we adopt photometric redshifts for the SXDF sample taken from Clements et al. (2008 – from optical-to-submm bands) and J. Furusawa et al. (in preparation – from optical-to-NIR bands). The optical-to-NIR photometric redshifts are calculated using a

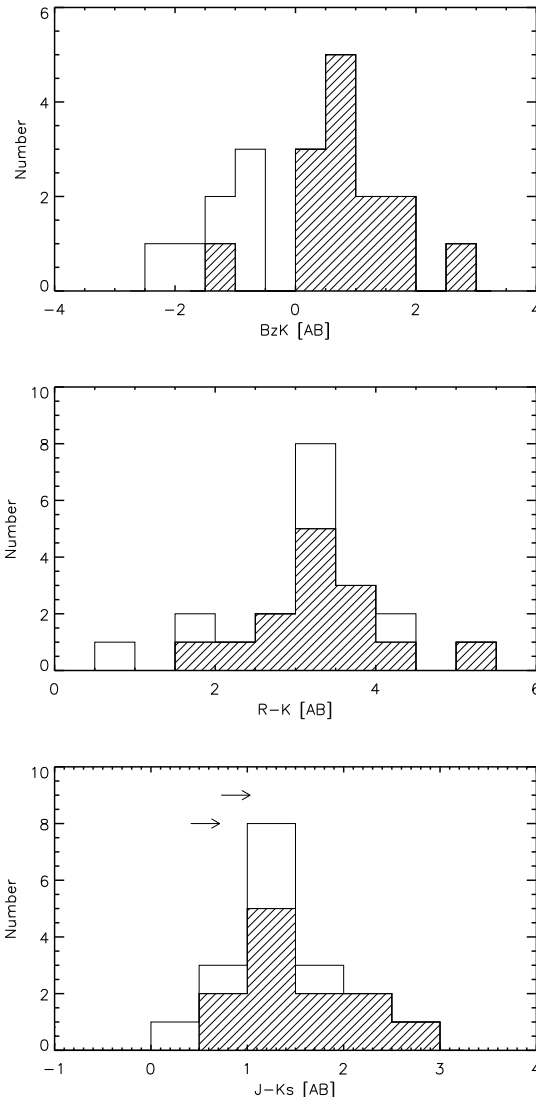


Figure 2. Histograms of BzK , $R-K$, and $J-K$ colours of singly associated SMGs in the SXDF. Hatched histograms indicate K -faint ($K_s > 21.3$) galaxies. Distribution of the BzK colour is bimodal, and almost all K -faint SMGs satisfy $BzK > -0.2$.

widely-used code HYPERZ³ (Bolzonella et al. 2000). This plot is remarkably similar to Figure 3. The BzK colours of SMGs indicate that the Balmer break of SMGs is strong enough to apply the BzK colour criteria to select SMGs at $1.4 \lesssim z \lesssim 2.5$.

In summary, our analysis suggests that K -faint SMGs are indeed an extreme subset of BzK galaxies at $1.4 < z < 2.5$, as originally speculated by Daddi et al. (2004). This result forms the basis of identifying SMGs using the BzK colours of associated NIR sources. In order to identify optical counterparts through specific galaxy populations (hereafter counterpart populations), such as radio sources and BzKs, the surface density of a counterpart population should be

³ We reject the best-fit solution if the corresponding probability is less than 1 per cent.

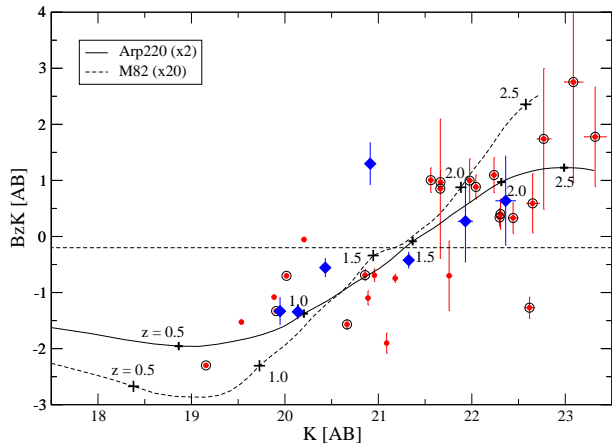


Figure 3. BzK colour versus K magnitude for radio-detected SMGs. Symbols are the same as in Figure 1. Solid and dashed lines indicate the BzK colours and magnitudes of Arp220 and M82 as a function of redshift. In order to match the SED templates of these two galaxies to the observed trend, their bolometric luminosities are multiplied by 2 and 20, resulting in 4×10^{12} and $8 \times 10^{11} L_{\odot}$ for Arp220 and M82, respectively.

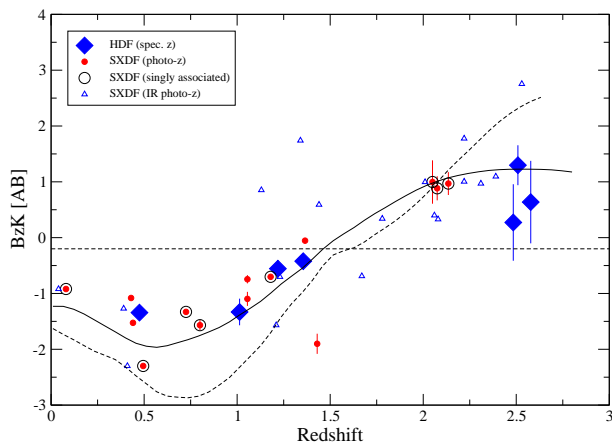


Figure 4. BzK colour versus Redshift for radio-detected SMGs. Symbols are the same as in Figure 3. Redshifts of the HDF sample (diamonds) are from spectroscopy. For the SXDF sample, we adopt photometric redshifts from optical-to-NIR bands (solid circles; Furusawa et al. in preparation) and from optical-to-submm bands (triangles; Clements et al. 2008).

low enough to ensure a small number of chance associations. If we use a counterpart population with a more confined colour space, the number of chance associations will be reduced. For this purpose, we focus not only on BzKs, but also on EROs and DRGs. Hereafter we refer to the BzK-ERO overlapping population as $RK/BzKs$ and the BzK-ERO-DRG overlapping population as $RJK/BzKs$.

3.2 Relation with EROs and DRGs

Figure 5 shows a colour-colour diagram with $R - K$ and $J - K$. The colour criteria for EROs and DRGs are indicated by dashed lines. The histograms of $R - K$ and $J - K$ of the singly associated SMGs are shown in Figure 2. Among the 20 singly associated SMGs, $40 \pm 10\%$ (8/20) are classified as

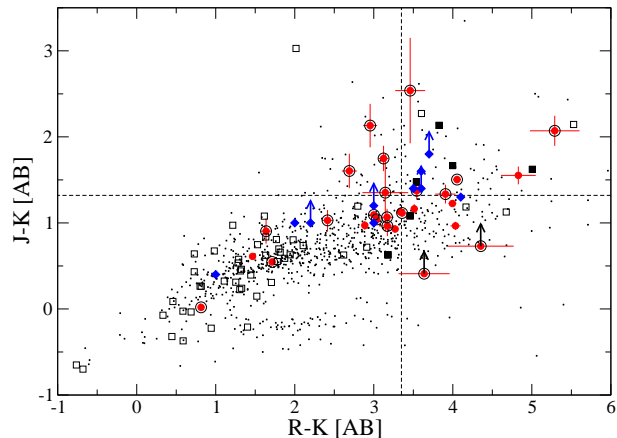


Figure 5. $J - K$ versus $R - K$ colour-colour diagram. Symbols are the same as in Figure 1.

EROs with $R - K > 3.35$. This fraction becomes $43 \pm 10\%$ (6/14) for the K -faint ($K_s > 21.3$) sample. On the other hand, the singly associated SMGs include 45 – 55% (9–11/20) of DRGs having $J - K > 1.3$. In the K -faint sample, there are 57 – 71% (8–10/14) of DRGs. The uncertainty in the DRG fraction comes from the J -band upper limits for two SMGs. There is no significant difference in $R - K$ and $J - K$ colours between the K -bright and K -faint samples. Thus, EROs and DRGs themselves are not as particularly useful as BzKs for optical identification.

We identify six $RK/BzKs$, all of which are singly associated SMGs. These galaxies have red $J - K_s$ colours satisfying the DRG selection criteria, although two sources have upper limits in the J band. Thus, about a half (6/13) of the BzK-selected SMGs are found to be EROs and DRGs, i.e. $RJK/BzKs$. As discussed in Takagi et al. (2007), this may mean that the duty cycle of extremely red SMGs is about a half of the SMG duty cycle. According to the radiative transfer SED model for starburst galaxies by Takagi et al. (2004), SMGs could have extremely red colours during the last half of the starburst phase because of evolved stellar populations.

4 OPTICAL IDENTIFICATION OF RADIO-UNDETECTED SMGs

Our analysis shows that almost all of the K -faint SMGs satisfy the BzK selection criteria $BzK > -0.2$. This gives strong support to perform ‘direct’ optical identification of SMGs using BzKs as a counterpart population, when there are no K -bright associations around SMGs. The overlapping populations, such as $RK/BzKs$ and $RJK/BzKs$, are useful to identify only a limited fraction of SMGs, but could give robust identifications because of lower surface densities. Using BzKs as a counterpart population, we employ the same identification procedure as in the radio identification (e.g. Ivison et al. 2002; Webb et al. 2003; Ivison et al. 2007), following the method proposed by Downes et al. (1986). With this method, we could identify radio-faint SMGs at $z \lesssim 2.5$. Such SMGs are expected to have a lower dust temperature than radio-detected SMGs at a similar redshift range (Chapman et al. 2005).

4.1 Method

The probability to find a physically unrelated object within a distance r of a given submm source may be described by $P_* = 1 - \exp(-\pi r^2 N_{\geq S_*})$, where $N_{\geq S_*}$ is the surface density of galaxies as bright as or brighter than the candidate identification with the flux of S_* . Downes et al. (1986) describe a correction to this raw Poisson probability, considering the contribution from very close associations of fainter sources ($S < S_*$) with a probability as low as $P \leq P_*$. The corrected probability can be written as $P' = 1 - \exp(-E)$ where $E = P_*[1 + \ln(P_*/P_c)]$, assuming $P \ll 1$. Here P_c is the critical probability to find a source brighter than the detection limit within the search radius. Because of a rather large search radius of $8''$ in our case, the values of P_* and P_c are not small enough to justify the assumption of $P \ll 1$. Therefore, we derive an equation valid even for $P \lesssim 1$: $E = y_*[1 + \ln(y_*/y_c)]$ where $y_{*,c} = -\ln(1 - P_{*,c})$.

Using the same optical-NIR catalogues as used for radio counterparts of SMGs, we search for K -band sources around the SHADES/SXDF sources with no robust radio counterparts with a search radius of $8''$. We have obtained 56 K -band sources around 24 radio-undetected SHADES sources. These sources are plotted as squares in the colour-colour diagrams shown in Figures 1 and 5. We regard BzKs in this sample as potential optical identifications of radio-undetected SMGs.

We calculate the corrected Poisson probability of chance associations by using the number counts of BzKs, RK /BzKs (Motohara et al. in preparation) and RJK /BzKs. Unfortunately, we find no galaxy counts for RJK /BzKs in the literature, while Takagi et al. (2007) show that $52 \pm 8\%$ (19/36) of RK /BzKs are DRGs at a magnitude limit of $K_s < 22.1$. Also Lane et al. (2007) report a fraction of $30 \pm 3\%$ (85/283) using a shallower ($K_s < 21.2$) but wider image. Here we assume that a half of RK /BzKs are DRGs, i.e. RJK /BzKs, at any magnitude bin. This fraction would give an upper limit on galaxy counts at the bright end. These counts are given up to $K_s = 23$. For galaxies fainter than this limit, we use the linearly extrapolated number counts in $\log N$ versus K magnitude. We summarise the surface density of each galaxy population with $K_s < 23$ in Table 2, including EROs and DRGs.

We calculate P' for each of the potential identifications, depending on the colour and the K_s -band total magnitude of the object under question. For each object, we adopt the minimum of P' for the final value P'_{NIR} . We regard galaxies with $P'_{\text{NIR}} < 0.1$ as tentative identification, and $P'_{\text{NIR}} < 0.05$ as being robust. In the presence of associations of K -bright sources, we regard any other association as a tentative identification even with $P' < 0.05$. This is because a half of SMGs are expected to be non-BzKs (see Section 3.1), and we have not ruled out the possibility of K -bright sources being the true counterparts.

Some SMGs are too faint to be detected in the K band. In Section 2.2, we find that $\sim 25\%$ of radio-detected SMGs have no counterparts in the K -band image. This fraction could be higher for radio-undetected SMGs, since they probably include a sub-sample of SMGs lying at the high redshift tail, i.e. $z \gtrsim 3$. We caution the readers that even robust BzK identifications are still plausible candidates, since we cannot rule out the possibility that true counterparts are not detected in the K band.

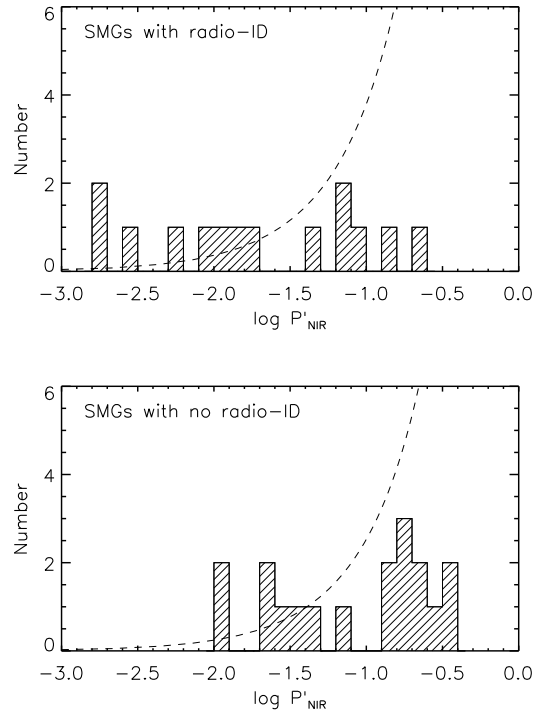


Figure 6. Histograms of P'_{NIR} for radio-detected SMGs and for BzKs around radio-undetected SMGs. Dashed line indicate the expected number of chance associations as a function of P' . See text in detail.

4.2 Results

Figure 6 shows the histogram of P'_{NIR} values for BzKs around the radio-undetected SMGs in the SXDF and also for the radio identifications. The radio identifications have a systematically lower P'_{NIR} than BzKs around the radio-undetected SMGs, owing to the pre-selection by radio with $P'_{\text{radio}} < 0.05$. The dashed lines in Figure 6 indicate the expected number of chance associations as a function of P' . The normalization of these curves is given by the number of searched regions, i.e. 36 for the SHADES sources with radio counterparts and 24 for those without radio counterparts.

In Table 3, we tabulate the derived P' for BzKs around the radio-undetected SHADES sources with $P'_{\text{NIR}} \leq 0.1$. The robust identifications are indicated by solid squares in the colour-colour diagrams (Figures 1 and 5). From the P' -statistics of NIR galaxies, we find 6 robust (including one double identification) and 2 tentative identifications. Thus, the success rate of identification is not very high, only $\sim 15\%$. This might be reasonable if we consider the possible bias in radio-undetected SMGs toward optically faint counterparts at high redshifts.

All of the robust NIR identifications but one are RK /BzKs or RJK /BzKs, owing to lower surface densities than that of bare BzKs. This indicates that the current positional uncertainty is too large to use bare BzKs for a counterpart population. Therefore, it is practical to use RK /BzKs and/or RJK /BzKs, although the completeness of identification would decrease by a factor of 2. This is still an encouraging performance for future exploitation. We can extend

Table 3. Optical identification of radio-undetected SMGs

NAME	R.A. [J2000]	Dec.	K_s [AB]	Dist. ^a [arcsec]	$P'_{BzK}{}^b$	$P'_{RK/BzK}{}^c$	$P'_{RJK/BzK}{}^d$
SXDF850.32	34.34489	-5.01260	22.55±0.06	7.46	0.292	0.076	0.039
SXDF850.39	34.46084	-4.92763	23.16±0.12	0.71	0.020
SXDF850.48	34.35387	-4.95468	22.99±0.09	4.66	0.244	0.057	0.029
SXDF850.56a ^e	34.45994	-5.10926	22.48±0.05	4.64	0.182	0.049	0.025
SXDF850.56b ^e	34.46235	-5.10814	21.44±0.02	4.96	0.071	0.023	0.012
SXDF850.70	34.54725	-5.04682	21.65±0.03	2.54	0.034	0.011	...
SXDF850.91 ^f	34.39587	-4.95518	23.31±0.14	6.08	0.319	0.075	...
SXDF850.93 ^f	34.38840	-4.96854	23.76±0.16	7.03	0.316	0.080	0.041

Note — Bold figures indicate the adopted P'_{NIR} . ^a Angular distance from SHADES centroid. ^b P' values for BzK galaxies. No entry indicates that the galaxy does not satisfy BzK colour criteria. ^c Same as ^b but for the BzK-ERO overlapping population. ^d Same as ^b but for the BzK-ERO-DRG overlapping population. ^e Two robust identifications for one SMG. ^f Tentative identification, because of $P' > 0.05$ (SXDF850.91) or the presence of another K -bright association (SXDF850.93).

this technique to higher redshifts, using a combination of photometric bands at longer wavelengths, such as RJL (see Daddi et al. 2004), zKM and so on. This technique will be useful to push the current ‘identification limit’ of SMGs to $z \gg 3$.

BzK-selected radio-undetected SMGs would have a lower dust temperature than radio detected ones. Although the sample suffers from various selection effects, due to optical-NIR colour cuts, we could put some constraints on the number of SMGs with cool dust. We identified 5 radio-undetected SMGs as BzKs. On the other hand, we found that 13 radio-detected SMGs (singly associated ones) are BzKs. Thus, we estimate that the fraction of radio-undetected SMGs at $1.4 \lesssim z \lesssim 2.5$ would be $\gtrsim 30\%$. This is a lower limit, since we can identify only SMGs with extremely red colours such as $RK/BzKs$ and $RJK/BzKs$. We also caution that our sample is limited to those with K -band magnitudes of $K_s \lesssim 23.5$, and missing extremely faint SMGs.

4.3 Fraction of SMGs in NIR galaxy populations

We summarise the fraction of SMGs in each NIR galaxy population by using the observed surface density. The effective area of SHADES in the SXDF is $\sim 250 \text{ arcmin}^2$ (Takagi et al. 2007). Considering both the radio and NIR identifications, we found 18(+1), 12(+4), and 12(+3) singly associated SMGs (plus possible candidates from multiple identifications) are BzKs, EROs, and DRGs, respectively⁴. These numbers give surface densities of SMGs with BzK, ERO, DRG colours of $0.07^{+0.02}_{-0.02}$, $0.05^{+0.03}_{-0.02}$, and $0.05^{+0.03}_{-0.02} \text{ arcmin}^{-2}$, respectively⁵. Using the surface density of each galaxy population in Table 2, we derive the fraction of SMGs in BzKs, EROs, and DRGs, to be about 1 per cent. These are the current best estimates of the fraction of SMGs in these galaxy populations.

Nine (6 radio and 3 NIR identified) singly associated

SMGs are found to be $RJK/BzKs$, giving a surface density of $\sim 0.04 \text{ arcmin}^{-2}$. The surface density of $RJK/BzKs$ would be around $0.25 - 0.7 \text{ arcmin}^{-2}$, considering the results by Takagi et al. (2007) and Lane et al. (2007). Thus, $\sim 10\%$ of $RJK/BzKs$ are likely to be SMGs, and therefore $RJK/BzKs$ contain a much higher fraction of SMGs than other optical/NIR-selected galaxy populations. This confirms the results by Takagi et al. (2007).

Given the assumed cosmology, a cosmic (co-moving) volume we consider is $9 \times 10^5 \text{ Mpc}^3$ for the redshift range of $1.4 < z < 2.5$ and the survey area of $\sim 250 \text{ arcmin}^2$. We find 18 BzK-selected SMGs in this volume, corresponding to a space density of $2 \times 10^{-5} \text{ Mpc}^{-3}$.

5 DISCUSSION

We discuss a possible evolutionary link between SMGs and BzKs and its implications for physical properties of SMGs, by using the star formation rate (SFR)-stellar mass (M_*) relation of BzKs. In the following, we discuss only SMGs satisfying the BzK selection criterion and $K < 20$ (Vega), in order to securely derive stellar masses. We find seven such SMGs (singly associated ones) from our sample. In order to increase the sample, we also use the sample of radio-detected SMGs in Chapman et al. (2005), which have spectroscopic redshifts and K -band photometry (Smail et al. 2004). We find seven SMGs in their sample, which have a starburst-dominated optical spectrum, a redshift at $1.4 \leq z \leq 2.5$ (i.e. the redshift range of BzKs), and $K < 20$ (Vega). We refer to this sample and the sample from the SXDF as the Chapman sample and the SXDF sample, respectively.

5.1 Are SMGs merging BzKs?

The starburst activity of SMGs seems to be induced by galaxy interactions/mergers as indicated by their morphology and dynamical properties (Chapman et al. 2004; Swinbank et al. 2006; Tacconi et al. 2006, 2008; Bouché et al. 2007). Immediate progenitors of SMGs would be gaseous star-forming galaxies as massive as SMGs. Most plausible candidates for this parent population would be star-forming

⁴ Here we count SXDF850.56 having two robust identifications as singly associated SMGs, since both are RJK/BzK .

⁵ The error includes a contribution from multiple identifications and that of survey area.

BzKs, given a similar stellar mass and coevality with SMGs. Although the SFRs of BzKs are sometimes as high as those of local ULIRGs (Daddi et al. 2005), the kinematical properties of BzKs are more similar to quiescent disc galaxies (Genzel et al. 2006; Bouché et al. 2007). This quiescent nature of star formation in BzKs is also supported by the measurement of the star formation efficiency from the CO luminosity, which is an order of magnitude lower than that of SMGs and similar to local spirals (Daddi et al. 2008). In the following discussion, we assume that some dynamical perturbations occurring in BzKs induce the vigorous star formation of SMGs.

5.2 SFR and stellar mass of SMGs

We derive the stellar masses of SMGs, using the empirical formulae by Daddi et al. (2004, their Eq. 6 and 7 for the SED-fitting-derived mass):

$$\log(M_*/10^{11} M_\odot) = -0.4(K^{\text{tot}} - K^{11}) + \Delta \log M_*, \quad (1)$$

$$\Delta \log M_* = 0.218[(z - K) - 2.29] \quad (2)$$

where $K^{11} = 19.51$ (Vega) is the K -band magnitude corresponding on average to a mass of $10^{11} M_\odot$. Since these formulae are calibrated for $K < 20$ (Vega), we restrict our sample of SMGs to those in this magnitude range as noted above. The correction term with $(z - K)$ colour is applied only for the SXDF sample, since z -band photometry is not available for the Chapman sample in the literature. The stellar masses derived from these formulae are based on the Salpeter initial mass function extending between 0.1 and $100 M_\odot$. In deriving the stellar masses, we adopt Petrosian magnitudes from the UKIDSS catalogue for estimation of total K -band magnitudes. For the Chapman sample, we adopt the total K -band magnitudes in Smail et al. (2004), which are estimated with the aperture photometry of a large ($4''$) diameter. We find that the mean stellar mass of 14 SMGs (7 from SXDF and the other 7 from the Chapman sample) is $1.2 \times 10^{11} M_\odot$. If we included SMGs with $K > 20$ (Vega) as well, the mean stellar mass would reduce about 20%. The uncertainty in the stellar mass on single objects is about 60% (Daddi et al. 2004). However, we caution that the uncertainty may be much larger than this, since SMGs would have a large fraction of mass in substantially obscured stellar populations. For example, Borys et al. (2005) derive on average 5 times higher stellar masses from rest-frame K -band magnitudes than those reported from modeling the UV/optical SEDs of SMGs in Smail et al. (2004).

The SFRs are derived from radio 1.4 GHz fluxes and redshifts. We estimate the FIR luminosities from the radio-infrared luminosity relation, $q_L = \log(L_{\text{FIR}}/\nu_0 L_{1.4 \text{ GHz}})$ found for SMGs (Kovács et al. 2006), where $q_L = 2.14$ and $\nu_0 = 4.52$ THz. The radio luminosities at the rest-frame 1.4 GHz are calculated with $L_{1.4 \text{ GHz}} = 4\pi D_L^2 S_{1.4} (1+z)^{\alpha-1}$ where D_L and $S_{1.4}$ are the luminosity distance and the 1.4 GHz flux density, and α is the spectral index ($S \propto \nu^{-\alpha}$). We adopt $\alpha = 0.7$ (Condon 1992). For the SXDF sample, we assume a redshift of $z = 1.9$, an average redshift of BzKs (Daddi et al. 2004). For the Chapman sample, we use the spectroscopic redshifts from Chapman et al. (2005). We convert the derived FIR luminosity to the SFR using a relation $\text{SFR} = L_{\text{FIR}}/5.8 \times 10^9 L_\odot$ (Kennicutt 1998). For the

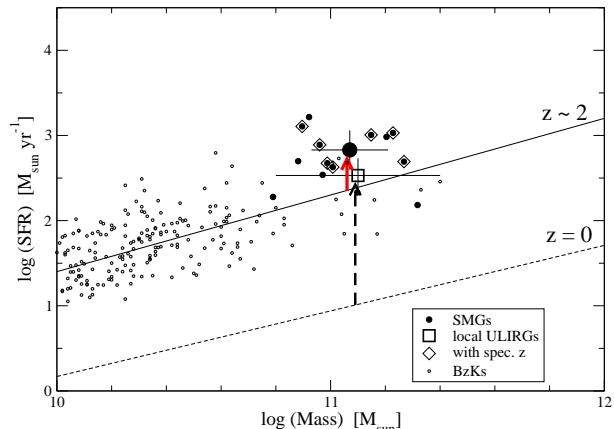


Figure 7. SFR vs. stellar mass of SMGs. For local ULIRGs we adopt the dynamical mass. Solid circles indicate SMGs. Solid circles inside diamonds indicate SMGs with spectroscopic redshifts. Open circles are for BzKs with $K < 22$ mag (Vega), taken from Daddi et al. (2007) with MIPS $24\mu\text{m}$ -based SFRs. The large solid circle indicates the average of SMGs, whose error bars represent the standard deviation of the combined SMG sample. The large open square corresponds to the average of local ULIRGs. Solid and dashed lines indicate the observed SFR-stellar mass relation of star-forming galaxies at $z \sim 2$ and 0, respectively. Solid and dashed arrows show a typical enhancement of SFR experienced by SMGs and local ULIRGs, respectively.

combined sample of SMGs, we derive an average SFR of $680 M_\odot \text{ yr}^{-1}$. This becomes $600 M_\odot \text{ yr}^{-1}$ if we include the SMGs with $K > 20$ (Vega). If we adopt the widely-used local radio-FIR relation by Condon (1992), instead of that for SMGs by Kovács et al. (2006), the derived SFRs increase by a factor of ~ 3 .

Local ULIRGs are also considered for comparison. We adopt the average of the sample in Tacconi et al. (2002). We use the dynamical mass, instead of the stellar mass, which gives a solid upper limit on the stellar mass. The averages of the dynamical masses and the SFRs are $1.3 \times 10^{11} M_\odot$ and $340 M_\odot \text{ yr}^{-1}$, respectively.

5.3 SFR enhancement of SMGs

We now consider how much SFRs are enhanced in SMGs, owing to dynamical perturbations. Such an enhancement may be estimated from a comparison of the average SFR of SMGs with that of BzKs, a suspected progenitor population of SMGs, with a similar stellar mass. We note that the increase in the stellar mass would be less than a factor of ~ 2 in merging of gas-rich galaxies to produce still gaseous SMGs, in which we could neglect the increase in stellar mass after merging. The average SFR of progenitor galaxies may be estimated from the correlation between SFRs and stellar masses found for BzKs or local star-forming galaxies, once we derive the stellar mass of SMGs or local ULIRGs.

In Figure 7, we plot the SFRs and stellar masses of SMGs and local ULIRGs. Daddi et al. (2007) present the correlation between the SFR and the stellar mass of BzKs, $\text{SFR} = 200 \times M_{11}^{0.9}$ where $M_{11} = 10^{11} M_\odot$, which is depicted as the solid line in the figure. Also, the same correlation but for local blue galaxies found in the Sloan Digital Sky Survey

– SFR = $8.7 \times M_{11}^{0.77}$ (Brinchmann et al. 2004; Elbaz et al. 2007) – is shown as the dashed line.

Comparing the average SFR and M_* of SMGs to the SFR- M_* relation of BzKs, we estimate that a typical enhancement of SFR experienced by SMGs is around a factor of 3 indicated as the solid arrow in Figure 7. This enhancement is rather moderate as if SMGs follow the same SFR- M_* relation. In the local universe, such a moderate enhancement is, for example, found for M82 (Figure 18 in Elbaz et al. 2007), whose starburst activity is likely to be induced by interactions with M81. Compared to local ULIRGs, this enhancement is less significant by an order of magnitude. We estimate the SFR enhancement of local ULIRGs to be a factor of ~ 30 (the dotted arrow), comparing the mean SFR and M_* of local ULIRGs with the SFR- M_* relation of local star-forming galaxies. This is a lower limit, since we use the dynamical mass for local ULIRGs. If progenitors of SMGs are BzKs with a stellar mass comparable to SMGs, then the SFR enhancement could *not* be as high as local ULIRGs. As Tacconi et al. (2006) indicated, SMGs are probably experiencing maximum starbursts (Elmegreen 1999), determined roughly by the dynamical time scale of galaxies and negative feedback due to super novae. The maximum SFR expected for SMGs would be around $600 M_\odot \text{yr}^{-1}$ (Tacconi et al. 2006), which is already comparable to the observed SFRs.

What are implications of a moderate ($3\times$) SFR enhancement of SMGs? In the local universe, such a moderate enhancement is found for typical interacting pairs of galaxies (not necessarily in the most luminous merging phase) with a projected distance of $r_p < 20$ kpc (Li et al. 2007). The numerical simulation by di Matteo et al. (2007) also indicates that a typical enhancement of SFR during the major merger phase is only a factor of < 5 . If this moderate enhancement is a typical case at $z \sim 2$ as well, the fraction of SMGs in star-forming BzKs could be as high as the merger fraction. Although the merger fraction at $z > 1$ is quite uncertain, it would be at least similar to or higher than the value at $z \lesssim 1$ of $\sim 10\%$ (e.g. Conselice et al. 2003; Lotz et al. 2008), because of the hierarchical clustering properties of the galaxy formation process. This argument leaves us an open question why the fraction of SMGs in BzKs is not > 10 per cent, but only ~ 1 per cent. A bias of the submm surveys, which tend to miss galaxies as luminous as SMGs but with higher dust temperatures, should play a role here, but the effect would be only a factor of ~ 2 (Chapman et al. 2004). Also we are missing some fraction of radio-undetected, and hence cool-dust SMGs, which are not extremely red (see Section 4.2). Even if we consider luminous dusty galaxies at $z \sim 2$ with both higher and lower dust temperatures, a correction for the incompleteness would be less than an order of magnitude, and therefore not enough to reconcile the apparent inconsistency.

We could explain this apparent inconsistency between the rareness of SMGs and its moderate SFR enhancement as follows. At $z \sim 2$, galaxy interactions may be too common, which means that high specific SFRs (mass-normalized SFRs) of BzKs are a result of galaxy interactions to some extent. In this case, there would be almost no net enhancement of SFR in typical interacting galaxies over the SFR- M_* relation. The SFR enhancement of SMGs looks moderate, but might be indeed significant as galaxies at $z \sim 2$, possi-

bly caused only by rare merging events, such as those with some particular orbit parameters, very equal mass ratios, or multiple mergers. For example, according to the numerical simulation by di Matteo et al. (2007), high gas concentrations and hence high SFR enhancement can be realized not in direct mergers, but in retrograde mergers.

We should bare in mind that SMGs are not the only galaxy population experiencing major mergers. SMGs will merely be a tip of iceberg. Law et al. (2007) suggest that UV morphologies of BzKs and UV-selected (BX/BM) galaxies are not distinguishable from that of SMGs. This indicates either that not only SMGs but also BzKs and BX/BM galaxies are experiencing merger-induced starbursts, or simply that the UV morphology is not a reliable indicator of a major merger. On the other hand, Bouché et al. (2007) show that SMGs are a dynamically distinctive galaxy population with large mass concentration, i.e. dynamically hotter than BzKs and BX/BM galaxies. Therefore, the UV morphology may not be very useful to identify dynamically hot galaxies at $z \gtrsim 2$, as suggested by no obvious correlations between the UV morphology and other galactic properties, such as SFR, outflow and stellar mass (Law et al. 2007). We need more direct measures on dynamical properties of galaxies at $z \sim 2$, in order to identify kin of SMGs. For this purpose, Atacama Large Millimeter Array (ALMA – Beasley et al. 2006) will play an important role, which is capable of measuring gas dynamics of ~ 1 -mJy sources, such as BzKs (Daddi et al. 2005).

6 SUMMARY

We identify optical-NIR counterparts of 28 radio-detected SMGs, including multiple associations, in the SHADES/SXDF, and have compiled optical and near-infrared photometry of these sources. We then investigate optical/near-infrared colours (BzK , $R - K$ and $J - K$) of radio-detected SMGs, along with the additional sample from the HDF, to find that almost all of K -faint ($K_s > 21.3$) SMGs have $BzK > -0.2$, i.e. BzKs. This forms a strong basis of identifying radio-undetected SMGs using BzKs around submm sources.

We calculate the formal significance (P' value) for individual BzKs around radio-undetected SMGs, and found 6 robust ($P' \leq 0.05$) identifications, including one double identification. All of these new identifications but one are extremely red, i.e. RK /BzKs or RJK /BzKs. It turns out that the current positional uncertainty is too large to use bare BzKs for the direct optical identification. However, this result is encouraging for future exploitation of SMGs at $z \gg 3$ using a combination of longer wavebands, such as RJL and zKM .

From a comparison of observed surface densities, we find that only ~ 1 per cent of BzKs, EROs and DRGs are SMGs, while this fraction is as high as $\sim 10\%$ for the BzK-ERO-DRG overlapping population, RJK /BzKs.

The average SFR of BzK-selected SMGs is $\sim 680 M_\odot \text{yr}^{-1}$. If SMGs are major mergers of typical disk-like star-forming galaxies at $z \sim 2$, i.e. BzKs, the enhancement of SFR occurring in SMGs would be only a factor of ~ 3 . This enhancement is an order of magnitude lower than that of local ULIRGs. Such a moderate en-

hancement of SFR is found in ordinary galaxy pairs with a separation of < 20 kpc in the local universe, and not significant at all. Thus, the rareness of SMGs at $z \sim 2$ is rather puzzling. This may be because the SFR of star-forming BzKs is already enhanced by galaxy interactions to some extent, and hence the moderate SFR enhancement of SMGs over BzKs could indeed be significant as a galaxy at $z \sim 2$. A quantitative explanation on statistical properties of ULIRGs near and far would be a challenging task for the theory of galaxy formation, requiring clear understanding of galaxy evolution and the physics of galaxy interactions.

ACKNOWLEDGMENTS

We thank all the members of the SHADES consortium for their persistent efforts to publish the source catalogue. We are grateful to K. Motohara for providing us the number counts of NIR-selected galaxies. Also we are thankful to J. Furusawa for providing us photometric redshifts from the SXDS. We wish to thank an anonymous referee for very useful and constructive comments, including the suggestion to add more samples from the literature. This work is based in part on data obtained as part of the UKIRT Infrared Deep Sky Survey and the Subaru/XMM-Newton deep survey. We thank D. Elbaz for providing us compiled spectral energy distributions of Arp220 and M82. We also thank E. Daddi for sending us his data points used in Figure 7. TT acknowledges the Japan Society for the Promotion of Science (JSPS – PD fellow, No. 18-7747).

REFERENCES

- Beasley A. J., Murowinski R., Tarenghi M., 2006, in *Ground-based and Airborne Telescopes*. Edited by Stepp, Larry M. Proceedings of the SPIE, Volume 6267, pp. 626702 (2006). Vol. 6267 of Presented at the Society of Photo-Optical Instrumentation Engineers (SPIE) Conference, The Atacama Large Millimeter/Submillimeter Array: overview and status
- Bertoldi F., Carilli C., Aravena M., Schinnerer E., Voss H., Smolcic V., Jahnke K., Scoville N., Blain A., et al. 2007, *ApJS*, 172, 132
- Blain A. W., Chapman S. C., Smail I., Ivison R., 2004, *ApJ*, 611, 725
- Blain A. W., Smail I., Ivison R. J., Kneib J.-P., Frayer D. T., 2002, *Phys. Rep.*, 369, 111
- Bolzonella M., Miralles J.-M., Pelló R., 2000, *A&A*, 363, 476
- Borys C., Scott D., Chapman S., Halpern M., Nandra K., Pope A., 2004, *MNRAS*, 355, 485
- Borys C., Smail I., Chapman S. C., Blain A. W., Alexander D. M., Ivison R. J., 2005, *ApJ*, 635, 853
- Bouché N., Cresci G., Davies R., Eisenhauer F., Förster Schreiber N. M., Genzel R., Gillessen S., Lehnert M., Lutz D., et al. 2007, *ApJ*, 671, 303
- Brinchmann J., Charlot S., White S. D. M., Tremonti C., Kauffmann G., Heckman T., Brinkmann J., 2004, *MNRAS*, 351, 1151
- Capak P., Cowie L. L., Hu E. M., Barger A. J., Dickinson M., Fernandez E., Giavalisco M., Komiyama Y., Kretschmer C., McNally C., Miyazaki S., Okamura S., Stern D., 2004, *AJ*, 127, 180
- Chapman S. C., Barger A. J., Cowie L. L., Scott D., Borys C., Capak P., Fomalont E. B., Lewis G. F., Richards E. A., Steffen A. T., Wilson G., Yun M., 2003, *ApJ*, 585, 57
- Chapman S. C., Blain A. W., Smail I., Ivison R. J., 2005, *ApJ*, 622, 772
- Chapman S. C., Richards E. A., Lewis G. F., Wilson G., Barger A. J., 2001, *ApJ*, 548, L147
- Chapman S. C., Smail I., Blain A. W., Ivison R. J., 2004, *ApJ*, 614, 671
- Chapman S. C., Smail I., Windhorst R., Muxlow T., Ivison R. J., 2004, *ApJ*, 611, 732
- Clements D., Eales S., Wojciechowski K., Webb T., Lilly S., Dunne L., Ivison R., McCracken H., Yun M., James A., Brodwin M., Le Fèvre O., Gear W., 2004, *MNRAS*, 351, 447
- Clements D. L., Vaccari M., Babbedge T., Oliver S., Rowan-Robinson M., Davoodi P., Ivison R., Farrah D., Dunlop J., et al. 2008, *ArXiv e-prints*, 803
- Condon J. J., 1992, *ARA&A*, 30, 575
- Conselice C. J., Bershady M. A., Dickinson M., Papovich C., 2003, *AJ*, 126, 1183
- Coppin K., Chapin E. L., Mortier A. M. J., Scott S. E., Borys C., Dunlop J. S., Halpern M., Hughes D. H., Pope A., et al. 2006, *MNRAS*, 372, 1621
- Coppin K., Halpern M., Scott D., Marsden G., Iwamuro F., Maihara T., Motohara K., Totani T., 2004, *MNRAS*, 354, 193
- Daddi E., Cimatti A., Renzini A., Fontana A., Mignoli M., Pozzetti L., Tozzi P., Zamorani G., 2004, *ApJ*, 617, 746
- Daddi E., Dannerbauer H., Elbaz D., Dickinson M., Morrison G., Stern D., Ravindranath S., 2008, *ApJ*, 673, L21
- Daddi E., Dickinson M., Chary R., Pope A., Morrison G., Alexander D. M., Bauer F. E., Brandt W. N., Giavalisco M., Ferguson H., Lee K.-S., Lehmer B. D., Papovich C., Renzini A., 2005, *ApJ*, 631, L13
- Daddi E., Dickinson M., Morrison G., Chary R., Cimatti A., Elbaz D., Frayer D., Renzini A., Pope A., Alexander D. M., Bauer F. E., Giavalisco M., Huynh M., Kurk J., Mignoli M., 2007, *ApJ*, 670, 156
- Dannerbauer H., Lehnert M. D., Lutz D., Tacconi L., Bertoldi F., Carilli C., Genzel R., Menten K. M., 2004, *ApJ*, 606, 664
- Dannerbauer H., Walter F., Morrison G., 2008, *ApJ*, 673, L127
- di Matteo P., Combes F., Melchior A.-L., Semelin B., 2007, *A&A*, 468, 61
- Downes A. J. B., Peacock J. A., Savage A., Carrie D. R., 1986, *MNRAS*, 218, 31
- Elbaz D., Daddi E., Le Borgne D., Dickinson M., Alexander D. M., Chary R.-R., Starck J.-L., Brandt W. N., Kitzbichler M., MacDonald E., Nonino M., Popesso P., Stern D., Vanzella E., 2007, *A&A*, 468, 33
- Elmegreen B. G., 1999, *ApJ*, 517, 103
- Frayer D. T., Reddy N. A., Armus L., Blain A. W., Scoville N. Z., Smail I., 2004, *AJ*, 127, 728
- Furusawa H., Kosugi G., Akiyama M., Takata T., Sekiguchi K., Tanaka I., Iwata I., Kajisawa M., Yasuda N., et al. 2008, *ArXiv e-prints*, 801
- Genzel R., Tacconi L. J., Eisenhauer F., Förster Schreiber N. M., Cimatti A., Daddi E., Bouché N., Davies R., Lehn-

- ert M. D., et al. 2006, *Nature*, 442, 786
- Hayashi M., Shimasaku K., Motohara K., Yoshida M., Okamura S., Kashikawa N., 2007, *ApJ*, 660, 72
- Iono D., Peck A. B., Pope A., Borys C., Scott D., Wilner D. J., Gurwell M., Ho P. T. P., Yun M. S., Matsushita S., Petitpas G. R., Dunlop J. S., Elvis M., Blain A., Le Floch E., 2006, *ApJ*, 640, L1
- Ivison R. J., Greve T. R., Dunlop J. S., Peacock J. A., Egami E., Smail I., Ibar E., van Kampen E., Aretxaga I., et al. 2007, *MNRAS*, 380, 199
- Ivison R. J., Greve T. R., Smail I., Dunlop J. S., Roche N. D., Scott S. E., Page M. J., Stevens J. A., Almaini O., Blain A. W., et al. 2002, *MNRAS*, 337, 1
- Kennicutt R. C., 1998, *ApJ*, 498, 541
- Kong X., Daddi E., Arimoto N., Renzini A., Broadhurst T., Cimatti A., Ikuta C., Ohta K., da Costa L., Olsen L. F., Onodera M., Tamura N., 2006, *ApJ*, 638, 72
- Kovács A., Chapman S. C., Dowell C. D., Blain A. W., Ivison R. J., Smail I., Phillips T. G., 2006, *ApJ*, 650, 592
- Lane K. P., Almaini O., Foucaud S., Simpson C., Smail I., McLure R. J., Conselice C. J., Cirasuolo M., Page M. J., Dunlop J. S., Hirst P., Watson M. G., Sekiguchi K., 2007, *MNRAS*, 379, L25
- Law D. R., Steidel C. C., Erb D. K., Pettini M., Reddy N. A., Shapley A. E., Adelberger K. L., Simenc D. J., 2007, *ApJ*, 656, 1
- Li C., Kauffmann G., Heckman T., Jing Y. P., White S. D. M., 2007, *ArXiv e-prints*, 711
- Lotz J. M., Davis M., Faber S. M., Guhathakurta P., Gwyn S., Huang J., Koo D. C., Le Floch E., Lin L., Newman J., Noeske K., et al. 2008, *ApJ*, 672, 177
- Maihara T., Iwamuro F., Tanabe H., Taguchi T., Hata R., Oya S., Kashikawa N., Iye M., Miyazaki S., et al. 2001, *PASJ*, 53, 25
- Mortier A. M. J., Serjeant S., Dunlop J. S., Scott S. E., Ade P., Alexander D., Almaini O., Aretxaga I., et al. 2005, *MNRAS*, 363, 563
- Nagayama T., Nagashima C., Nakajima Y., Nagata T., Sato S., Nakaya H., Yamamuro T., Sugitani K., Tamura M., 2003, in *Instrument Design and Performance for Optical/Infrared Ground-based Telescopes*. Edited by Iye, Masanori; Moorwood, Alan F. M. *Proceedings of the SPIE*, Volume 4841, pp. 459-464 (2003). SIRUS: a near infrared simultaneous three-band camera. pp 459-464
- Pope A., Borys C., Scott D., Conselice C., Dickinson M., Mobasher B., 2005, *MNRAS*, 358, 149
- Priddey R. S., Ivison R. J., Isaak K. G., 2008, *MNRAS*, 383, 289
- Reddy N. A., Erb D. K., Steidel C. C., Shapley A. E., Adelberger K. L., Pettini M., 2005, *ApJ*, 633, 748
- Serjeant S., Farrah D., Geach J., Takagi T., Verma A., Kaviani A., Fox M., 2003, *MNRAS*, 346, L51
- Smail I., Chapman S. C., Blain A. W., Ivison R. J., 2004, *ApJ*, 616, 71
- Smail I., Ivison R. J., Blain A. W., Kneib J.-P., 2002, *MNRAS*, 331, 495
- Smail I., Ivison R. J., Kneib J.-P., Cowie L. L., Blain A. W., Barger A. J., Owen F. N., Morrison G., 1999, *MNRAS*, 308, 1061
- Swinbank A. M., Chapman S. C., Smail I., Lindner C., Borys C., Blain A. W., Ivison R. J., Lewis G. F., 2006, *MNRAS*, 371, 465
- Tacconi L. J., Genzel R., Lutz D., Rigopoulou D., Baker A. J., Iserlohe C., Tecza M., 2002, *ApJ*, 580, 73
- Tacconi L. J., Genzel R., Smail I., Neri R., Chapman S. C., Ivison R. J., Blain A., Cox P., Omont A., et al. 2008, *ArXiv e-prints*, 801
- Tacconi L. J., Neri R., Chapman S. C., Genzel R., Smail I., Ivison R. J., Bertoldi F., Blain A., Cox P., Greve T., Omont A., 2006, *ApJ*, 640, 228
- Takagi T., Hanami H., Arimoto N., 2004, *MNRAS*, 355, 424
- Takagi T., Mortier A. M. J., Shimasaku K., Coppin K., Pope A., Ivison R. J., Hanami H., Serjeant S., Clements D. L., et al. 2007, *MNRAS*, 381, 1154
- Takagi T., Vasevicius V., Arimoto N., 2003, *PASJ*, 55, 385
- Wang W.-H., Cowie L. L., van Sadlers J., Barger A. J., Williams J. P., 2007, *ApJ*, 670, L89
- Warren S. J., Hambly N. C., Dye S., Almaini O., Cross N. J. G., Edge A. C., Foucaud S., Hewett P. C., Hodgkin S. T., Irwin M. J., Jameson R. F., Lawrence A., Lucas P. W., Adamson A. J., et al. 2007, *MNRAS*, 375, 213
- Webb T. M. A., Lilly S. J., Clements D. L., Eales S., Yun M., Brodwin M., Dunne L., Gear W. K., 2003, *ApJ*, 597, 680
- Younger J. D., Fazio G. G., Huang J.-S., Yun M. S., Wilson G. W., Ashby M. L. N., Gurwell M. A., Lai K., Peck A. B., et al. 2007, *ApJ*, 671, 1531